Role of the glycoprotein thorns in anxious effects of rabies virus: Evidence from an animal study

Soheil Ghassemi, Hamid Gholami Pourbadie, Christophe Prehaud, Monique Lafon, Mohammad Sayyah

Role of the glycoprotein thorns in anxious effects of rabies virus: Evidence from an animal study

Soheil Ghassemi[1], Hamid Gholami Pourbadie[1*], Christophe Prehaud[2], Monique Lafon[2], Mohammad Sayyah[1*]

[1]Department of Physiology and Pharmacology, Pasteur Institute of Iran, Tehran, Iran

[2]Institut Pasteur, Unité de Neuroimmunologie Virale, UMR 3569, CNRS, Paris, France

** Corresponding authors: h_gholamipour@pasteur.ac.ir (HG. Pourbadie), sayyahm2@pasteur.ac.ir (M. Sayyah)*

Role of the glycoprotein thorns in anxious effects of rabies virus: Evidence from an animal study

ABSTRACT

Rabies is a lethal infectious disease caused by rabies virus (RABV). Fear and anxiety are the distinguished symptoms in rabies patients. Fusion of RABV envelope glycoprotein (RVG) to host cell membrane initiates rabies pathogenesis via interacting with PDZ domain of signaling proteins. We assessed the anxiety-like behaviors, and hypothalamic–pituitary–adrenal axis (HPA) response to RVG infection. Contribution of PDZ binding motif (PBM) of RVG to the observed effects was also examined using a mutant form of RVG, ΔRVG, with deleted last four amino acids at PBM C-terminus. Lentiviral vectors containing RVG and/or ΔRVG genes were injected into the rat brain areas involved in anxiety including hypothalamus, dorsal hippocampus, and amygdala. RVG/ΔRVG neural expression was examined by fluorescent microscopy. Anxiety-like behaviors were assessed by elevated plus maze (EPM) and open field (OF) tasks. HPA response was evaluated via measuring corticosterone serum level by ELISA technique. RVG/ΔRVG were successfully expressed in neurons of the injected areas. RVG, but not ΔRVG, Infection of hypothalamus and amygdala increased the time spent in EPM open arms, and OF total distance moved and velocity. RVG, but not ΔRVG, infection of hypothalamus and dorsal hippocampus increased corticosterone level. The anxiety-like behaviors and exploratory/locomotor activities of rats with RVG infection in hypothalamus, and amygdala are mediated by PBM of RVG. The HPA response to RVG infection of hypothalamus and dorsal hippocampus is dependent to PBM of RVG.

Triggering anxiety-related signaling by PBM of RVG seems to be one of the mechanisms involved in anxiety behaviors seen in patients with rabies.

Keywords: Corticosterone; Elevated plus maze; PBM; Rabies envelope

1. Introduction

Rabies is a zoonotic, viral disease accompanied by almost always fatal encephalomyelitis. There are two forms of the disease, Furious rabies and Paralytic rabies. Furious rabies account for about 80% of the total number of human cases. The initial symptoms include a fever with pain and paresthesia at the bite wound. As the virus enters the central nervous system, typically 2–3 months after an encounter with a rabid animal (may vary from 1 week to 1 year dependent upon factors such as the location of virus entry and viral load), progressive and fatal inflammation of the brain and spinal cord develops. Intense anxiety and nervousness, hydrophobia (fear of water) and sometimes aerophobia (fear of drafts or of fresh air) emerge. Once clinical symptoms appear, rabies is virtually 100% fatal. Convulsive seizures and progressive paralysis follows, and within a few days the patient dies in coma (Mitrabhakdi et al., 2005). Rabies is caused by rabies virus (RABV). RABV is a bullet shape Rhabdovirus with high affinity to nerve cells. The virus is composed of an internal protein core or nucleocapsid comprising the nucleic acid, and an external envelope, a lipid-containing bilayer roofed with transmembrane glycoprotein spines (Koury and Warrington, 2021). RABV genome encodes five proteins organizing either the ribonucleoprotein (RNP) complex or the viral envelope (Tordo and Kouknetzoff 1993). The L (transcriptase), N (nucleoprotein), and NS (transcriptase-associated) proteins comprise the RNP complex, together with the viral RNA. These components aggregate in the cytoplasm of virus-

infected neurons and compose Negri bodies, the distinctive histopathologic finding of RABV infection (Albertini et al., 2011). The G (glycoprotein) and M (matrix) proteins form the lipid envelope. The G protein erects the thorns that cover the outer surface of the virion envelope. These transmembrane glycoprotein spines bind specifically to cellular receptor and confirm neurotropism in infected cells (Rupprecht, 1996).

PDZ domains [named for the common structural domain shared by the postsynaptic density protein (PSD95), Drosophila disc large tumor suppressor (DlgA), and zonula occludens-1 protein (ZO-1)], are protein-protein interaction elements involved in cellular and biological functions, particularly signal transduction (Kennedy, 1995). They typically recognize and bind to a short region of the carboxy-termini of target proteins (Saras and Heldin, 1996). PDZ domains are typically found in cytoplasmic and membrane adapter proteins. The peptide sequence that binds to a PDZ domain is referred to as the PDZ domain-binding motif, or PBM. RABV encodes proteins with PBMs that target a particular set of the PDZ proteins. The association of viral PBMs with their PDZ protein targets results in modulation of the cellular processes involved in viral pathogenesis (Javier and Rice, 2011). The survival or death of RABV-infected neurons depends on the type of cellular PDZ proteins which are able to bind the PBM at the C-terminus of viral envelope glycoprotein. The full-length RABV G-protein (RVG) is a 524-amino acids type I glycoprotein (Fig. 1). RVG is attached to the endoplasmic reticulum (ER) and plasma membranes via its unique transmembrane domain and signal peptide. The ectodomain of RVG is initially located within the luminal compartment of the ER, and then at the cell surface after fusion to the plasma membrane. During G-protein trafficking from the ER to the plasma membrane, the cytoplasmic domain containing the

C-terminal PBM is always exposed to the cytoplasm of the somato-dendritic neuronal area, where it can interact with cellular partners. By modifying the length of RVG, some peptides are derived with increased affinity for PDZ domain and altered biological activity (Khan et al., 2019). ΔRVG (Fig. 1) is one of these modified peptides similar to RVG, which lacks the last four amino acids at the C-terminus of the PBM (Khan et al., 2019).

There are plenty of evidence indicating that RABV alters function of neurons by affecting neural ion channels, neurotransmitter release, and signaling receptors (Fu and Jackson 2005). However, very little pathological changes including neurodegeneration and neuroinflammation have been observed in the brain of rabies patients (Baloul and Lafon, 2003; Scott et al., 2008; Lafon, 2011; Rossiter and Jackson, 2020). In line with these evidence we have recently shown that infecting rat brain with RVG increases synaptic transmission in the hippocampus and strengthens spatial as well as fear-related memories (Ghassemi et al., 2021a, 2021b). We found that the PBM of RVG contributes to these electrophysiological and behavioral observations, without generating any histopathological or neuroinflammatory changes in the hippocampus (Ghassemi et al., 2021a, 2021b).

Anxiety and fear are well known symptoms seen in the rabies patients (Lindtjørn, 1982). Hypothalamus is the remarkable brain region involved in fear response (Steimer, 2002). Meanwhile, hippocampus and amygdala have a key role in modulating fear and anxiety. The limbic system structure, hippocampus controls hypothalamic stress-response system and exerts negative feedback to hypothalamic–pituitary–adrenal (HPA) axis. In addition, the evolutionarily ancient limbic system structure, the amygdala

is responsible for the expression of fear and aggression as well as species-specific defensive behaviors, and formation and retrieval of emotional and fear-related memories (Martin et al., 2009).

In line with the previous studies substantiating the role of RVG in the behavioral changes seen in rabies, we supposed that RVG might also contribute to the anxiety behaviors via interaction of its PBM with the PDZ of neural cells. Therefore, we assessed the anxiety-like behaviors and HPA axis response of rats with RVG and/or ΔRVG infection in hypothalamus, dorsal hippocampus, and amygdala.

2. Materials and methods

2.1. Lentiviral vector production and titration

Two lentiviral vectors encoding RVG, and or ΔRVG of challenge virus standard (Fig.1) were constructed according to the previously described method (Ghassemi et al., 2021b). Briefly, HEK 293T cells were cultured in Dulbecco's Modified Eagle Medium (DMEM, with 10 % FBS and 100units/ml penicillin/streptomycin) under 37 °C and 5 % CO2 incubation. Plasmids encoding either full-length RVG of challenge virus standard CVS (G-CVS) or ΔRVG were kindly provided by Christophe Prehaud (Neuroimmunologie Virale, Institute Pasteur, Paris, France) and sub-cloned in Plenti7.3 with eGFP genome (Invitrogen, France) containing cytomegalovirus (CMV) promoter. The HEK 293T cells were transfected with envelope (G protein of VSV), transfer (p-Lenti-G-CVS) and packaging (pMDLg, pRRE and pRSV/Rev) plasmids by calcium phosphate method. After 24 h, the medium was replaced by fresh medium containing 2 % FBS and the cells were incubated for 48 h. The medium was then collected by 5 min

centrifugation at 1000 ×g and 4 ℃. The supernatant was filtered through a 0.45 µm poly ether sulfone filter. Viral particles were then centrifuged at 50000×g and 4 ℃ for 2 h. The pellet was suspended in phosphate-buffered saline (PBS)-BSA 1 % solution. Different aliquots were then prepared and kept in $-80℃$ until use. In order to determine virus titration, the overnight cultured HEK 293T cells were transduced by the serial dilutions of the lentiviral vector. Number of GFP-positive cells in each dilution was determined under a fluorescent microscope (Nikon, Japan) at the day 3. The functional vector titer (transducing units, TU) was measured using the following formula:

Titer / (TU/ ml) = [GFP-positive cells × number of cells on the transduction day (5×10^5)]/dilution

2.2. Animals and Stereotaxic surgery

Adult male Wistar rats (220 g to 250 g, Pasteur Institute of Iran, n = 134) were used in this study. Experiments were adjusted in accordance with the Review Board and Ethics Committee of Pasteur Institute of Iran (Authorization code 93-0201-785, 22 April 2014) and conform to Council Directive 2010/63EU of the European Parliament, and the Council of 22 September 2010 on the protection of animals used for scientific purposes. Rats were anesthetized by ketamine (100 mg/kg, i.p.) and xylazine (10 mg/kg, i.p.). Intracranial injection was performed by stereotaxic surgery. Briefly, 2µl PBS or lentivirus containing RVG or ΔRVG, was delivered bilaterally into hypothalamic PVN (AP = – 1.7, ML= ± 0.4, DV= – 7.8), or dorsal hippocampus (AP= - 3.6, ML= ± 2, DV= - 2.2), or amygdala (AP= – 1.4, ML= ± 3.5, DV= – 5.1) through a Hamilton microsyringe connected to microinfusion pump, according to coordinates of the atlas of rat brain (Paxinos and Watson, 2006).

137 *2.3. Histology*

138 The presence of GFP-positive cells was examined in the injected area one week or two
139 weeks after intracranial microinjection of the lentivector according to the previously
140 described method (Ghassemi et al., 2021b). Briefly, rats were anesthetized and
141 perfused transcardially with 4 % paraformaldehyde. Brains were then removed, post-
142 fixed in 2 % paraformaldehyde, processed and embedded in paraffin blocks. Using a
143 microtome, the brains were horizontally sliced into 5 µm thickness. The sections were
144 mounted with 90 % glycerol/PBS buffer and observed in the dark room under
145 fluorescent microscope (Nikon, Japan) equipped with specific filter cube for FITC
146 fluorescence channels. Digital photographs were taken using 10x and 20x objective
147 lenses.

148 *2.4. Elevated plus maze task*

149 Elevated plus maze (EPM) was a plus shape apparatus elevated 50 cm above the
150 ground. It consisted of two open arms (45 cm × 10 cm long and width, respectively), two
151 enclosed arms (45 cm × 10 cm × 30 cm, long, width and high respectively), and a
152 middle compartment (10 cm × 10 cm). Thirty min before starting the test, rats were
153 moved to the testing room under dim light in order to familiarization. Each rat was
154 positioned in the middle compartment while it was facing to an open arm and permitted
155 to freely search the maze for 5 min. Ethanol 70 % was used to clean the maze after
156 each 5 min run. Locomotion was recorded by a CCD camera (Panasonic Inc, Japan)
157 hanging from the ceiling above the maze, digitized and saved to the computer by a
158 video tracking software (Ethovision, versionXT7, The Netherlands). The duration / s
159 spent in the open and enclosed arms was recorded. The parameters of percentage of

time elapsed in enclosed and open arms, percentage of enclosed arms entries and total distance moved were analyzed.

2.5. Open field test

Locomotor and exploratory activity of rats was measured by an open field (OF) apparatus (75 cm × 75 cm × 40 cm). Rats were placed individually into the center of the field, and the total distance during 20 min was recorded by the CCD camera.

2.6. Measuring corticosterone serum level

One week after microinjection of lentivectors or vehicle, animals were anesthetized with ketamine and xylazine. The arterial blood was collected via inserting a 23 gauge needle into the left ventricle. Serum was obtained by 3000 ×g centrifugation of blood samples for 5 min. Then the serum samples were maintained at –20 °C until use. Corticosterone concentration in serum was measured using a commercial rat corticosterone ELISA kit (ZellBio GmbH, Germany) according to the instructions of the manufacturer.

2.7. Experimental design

Experimental design of the study is presented in Fig. 2. Two main experiments were designed. First experiment (Fig. 2A) comprised 3 sub-experiments with 3 groups in each. The lentiviral vectors or vehicle were microinjected into the paraventricular nucleus (PVN) of hypothalamus (sub-experiment # 1, n = 42), or dorsal hippocampus (sub-experiment # 2, n = 21), or basolateral amygdala (BLA, sub-experiment # 3, n = 21). Three groups in each sub-experiment were allocated as control, RVG, and ΔRVG (7 rats in each group) in which animals received PBS, or lentivector containing RVG or ΔRVG through stereotaxic microinjection. Rats with intra-PVN microinjections are

182 divided into two subgroups (21 rats in each subgroup). OF as well as EPM tests
183 performed one week (Day 7 and Day 8, respectively) and two weeks (Day 14 and Day
184 15, respectively) after microinjections. In sub-experiments # 2 and # 3, OF and EPM
185 tasks performed only at one week (Day 7 and Day 8, respectively) post-injection period.
186 After performing the tasks, the brain of the animals was dissected out for histological
187 analyses. In the second main experiment (Fig. 2B), the 3 sub-experimental groups (4
188 rats in each group) received lentiviral vectors (RVG or ΔRVG) or vehicle intra PVN, or
189 intra dorsal hippocampus, or intra BLA. The serum level of corticosterone was
190 measured one week thereafter. In order to assess proper functioning of EPM test and
191 HPA response, two more groups were allocated as naïve control (n = 7), and positive
192 control (caffeine 60 mg/kg, i.p., n = 7) groups (Fig. 2C). Thirty min after the injection
193 EPM task performed. Then, the serum level of corticosterone was measured.

194 *2.8. Data analysis*

195 The data are expressed as Mean ± SEM and processed by Graph Pad Prism 6.0.
196 Kolmogorov-Smirnov test was used to check the normal distribution of the data. The
197 data with normal distribution were analyzed by the Un-paired student's *t*-test or One-
198 way analysis of variance (ANOVA) with Tukey post-hoc test. The data of corticosterone
199 level in the hypothalamus, amygdala, and caffeine experiments did not follow a normal
200 distribution. Therefore, they were analyzed by the nonparametric Kruskal-Wallis test
201 followed by Dunn's multiple comparisons test. In all cases, a $P \leq 0.05$ was considered
202 statistically significant.

203 **3. Results**

A titer of 10^8 transduction units/ml was obtained consistently.

3.1. Caffeine induced anxiety-like behaviors in elevated plus maze test

Fig. 3 demonstrates the caffeine effect on EPM task. The Un-paired student's *t*-test revealed that caffeine caused rats spent less time in the open arms (Fig. 3A, $P < 0.001$ compared to control). They also showed less entries to the open arms ($P < 0.01$ compared to control, Fig. 3B). This data indicate that our EPM set up works properly, and truly shows the anxiety-like state of rats.

Caffeine also induced longer distance moved (Fig. 3C) and greater number of total entrance to the both close and open arms (Fig. 3D) in contrast to the control group ($P < 0.0001$ and $P < 0.05$, respectively). These findings show positive impact of caffeine on motor behavior. Non-parametric Kruskal Wallis test followed by Dunn's multiple comparisons test revealed that exposure to EPM did not change corticosterone level of rats (Fig. 3E). However, caffeine could significantly increase corticosterone level ($P < 0.01$ compared to control Fig. 3E).

3.2. Expression of RVG in hypothalamic PVN induced anxiety-like behaviors

Fig. 4 shows the schematic loci of rat hypothalamic PVN (Fig. 4A) and green cells expressing RVG (Fig. 4 B and C) or ΔRVG (Fig. 4 D and E) indicating successful expression of GFP/RVG or GFP/ΔRVG in PVN one week after microinjection of the lentivector.

The corticosterone serum level of the experimental groups one week after injection of the lentivectors is demonstrated in Fig. 4F. Rats expressed RVG in PVN had a significantly higher corticosterone level compared to control group ($P < 0.05$). However,

ΔRVG expression in PVN could not significantly change the corticosterone level compared to control rats. The difference in corticosterone level between RVG- and ΔRVG-infected rats was not significant ($P > 0.05$).

Analysis of the OF task revealed no significant difference in the time spent in the center zone among groups at one week post-infection period (Fig. 4G). One way ANOVA revealed a significant difference in the entire distance moved among groups one week after lentivector injection ($F (2, 14) = 10.43$, $P = 0.001$). As depicted in Fig. 4H, rats in RVG group traveled longer distance than control group ($P < 0.01$). However, rats expressing ΔRVG moved less distance than RVG group ($P < 0.001$). No significant difference was found between control and ΔRVG group in the traveled distance. The difference in the ratio of entrances from center to the surround was not significant among the experimental groups at one week after lentivector injection (Fig. 4I). Fig. 4J shows locomotion speed of rats expressing RVG/ΔRVG in the PVN. At one week after lentivector injection, RVG-expressed rats showed higher velocity than control ($P < 0.05$) and ΔRVG ($P < 0.01$). No significant difference was found between ΔRVG and control groups.

Fig.4 K-N show the EPM data one week after delivering RVG/ΔRVG containing lentiviral vectors into the PVN. One way ANOVA revealed a significant difference in the time elapsed in the enclosed arms among groups ($F (2, 22) = 9.560$, $P = 0.001$). Tukey post-test demonstrated that rats expressing RVG in the PVN spent more time in the enclosed arms at one week (Fig. 4K) after lentivector injection ($P < 0.001$, compared to control group). The preference to remain in the enclosed arms in rats expressing ΔRVG was similar to the control group with no significant difference. The difference between ΔRVG

and RVG groups in the duration remaining in the enclosed arms was significant ($P < 0.001$, Fig. 4K). The percentage of time spent in the open arms was also significantly different among groups ($F (2, 17) = 32.10$, $P < 0.0001$) at one week post infection. Rats expressing RVG in the PVN spent less time in the open arms ($P < 0.0001$, compared to control group, Fig. 4K). Significant differences were also found between RVG and ΔRVG ($P < 0.01$) groups. No significant difference in the enclosed and open arm entries (Fig. 4L), the total distance moved (Fig. 4M) and the total number of entrances to the arms were found between groups at one week post-infection (Fig. 4N).

Two weeks after microinjection of the lentivector into PVN, RVG (Fig. 5 A and B) or ΔRVG (Fig. 5 C and D) was successfully expressed. No significant difference was found among groups in the time spent in the OF center zone (Fig. 5E). One way ANOVA revealed a significant difference in the total distance moved among groups ($F (2, 17) = 4.644$, $P = 0.0246$). RVG expressing rats traveled longer distance in the OF task compared to the control group ($P < 0.05$, Fig. 5F). No significant difference in the center to corner entrance ratio was found among groups in the OF test at two weeks post-infection (Fig. 5G). There was also no significant difference in the locomotion speed of the experimental groups at two weeks after lentivector injection into PVN (Fig. 5H).

Fig. 5I-L show EPM task two weeks after lentivector injection into PVN. One way ANOVA showed a significant difference in the time elapsed in enclosed arms among the groups ($F (2, 14) = 16.40$, $P = 0.0002$). Tukey post-test revealed that rats expressing RVG in the PVN spent more time in the enclosed arms ($P < 0.01$, Fig. 5I). No significant difference in the preference to remain in the enclosed arms was found between control and ΔRVG group. The difference between ΔRVG and RVG groups in the duration

remaining in the enclosed arms was significant ($P < 0.001$, Fig. 5I). The time spent in the open arms was also significantly different among groups ($F (2, 17) = 31.37$, $P < 0.0001$) at two weeks post-infection period. RVG group spent less time in the open arms ($P < 0.001$, compared to control group, Fig. 5I). Significant differences were also found between RVG and ΔRVG ($P < 0.001$) groups. No significant difference in the enclosed and open arms entries (Fig. 5J), the travelled distance (Fig. 5K) and the total arms entries (Fig. 5L) were found between groups at two weeks post-infection period.

3.3. Expression of RVG in dorsal hippocampus did not induce anxiety-like behaviors

Fig. 6A shows schematic coronal section of the dorsal hippocampus in rats. The representative fluorescent images of dorsal hippocampus one week after microinjection of the lentivector containing RVG or ΔRVG are presented in Fig. 6B-C and Fig. 6D-E, respectively. Green fluorescent cells indicate successful expression of RVG/GFP or ΔRVG/GFP in CA1 and dentate gyrus regions (Fig. S1).

The serum corticosterone level of the experimental groups is demonstrated in Fig. 6F. One way ANOVA showed different concentration of the corticosterone among the groups ($F (2, 15) = 9.89$, $P = 0.0018$). Corticosterone level significantly increased in both RVG and ΔRVG groups compared to the control ($P < 0.01$). No significant difference was found between RVG and ΔRVG groups.

Fig. 6G-J show the OF task in the experimental groups. One way ANOVA revealed a significant difference in the time spent in the center zone among groups ($F (2, 15) = 16.04$, $P = 0.0002$). Rats expressing RVG and ΔRVG in dorsal hippocampus spent less time in the center zone compared to the control ($P < 0.001$and $P < 0.01$, respectively) group (Fig. 6G). No significant difference in the entire traveled distance (Fig. 6H) and

the speed of movement (Fig. 6J) was found between groups. Rats expressing RVG and ΔRVG showed significant decrease in the center to the surround entrance ratio compared to the control group ($F(2, 20) = 4.236$, $P < 0.05$, Fig. 6I).

The lowest panel shows EPM task in the experimental groups. Rats expressing RVG in the dorsal hippocampus remained mainly in the enclosed arms (Fig. 6K, $P < 0.05$ compared to control group). No difference was found between ΔRVG and control group in the time spent in enclosed arms. There was significant difference between RVG and ΔRVG in the time remaining in the enclosed arms ($P < 0.001$). No significant difference was found among the experimental groups in the time spent in the open arms (Fig. 6K). Also, there was no significant difference in percentage of entries to the enclosed and open arms among groups (Fig. 6L). One-way ANOVA showed a significant difference in the total distance moved among groups ($F(2, 20) = 4.925$, $P = 0.0182$). RVG and ΔRVG expressing rats traveled longer distance compared to the control group ($P < 0.05$, Fig. 6M). However, no significant difference in the total arm entries was found between RVG and ΔRVG groups (Fig. 6N)

3.4. Expression of RVG in amygdala induced anxiety-like behaviors

Fig. 7A shows schematic coronal section of the amygdala region. Green fluorescent cells in the amygdala one week after microinjection of the lentiviral vectors indicate expression of GFP/RVG and GFP/ΔRVG in the amygdala (Fig. 7B-C and D-E, respectively). Non-parametric analysis via Kruskal-Wallis test revealed no significant difference in corticosterone level among experimental groups ($P = 0.1668$, Fig. 7F).

Fig. 7G-J show the OF task. Rats expressing RVG in amygdala spent less time in the center zone compared to the control ($P < 0.05$) and ΔRVG ($P < 0.05$) group ($F(2, 16) =$

318 5.617, P = 0.0142, Fig. 7G). RVG expressing rats travelled longer distance than control
319 (P < 0.001) and ΔRVG (P < 0.05) group in the OF test (F (2, 16) = 10.65, P = 0.0011,
320 Fig. 7H). No significant difference in the center to surround entrance ratio was found
321 among groups (Fig. 7I). Intra-amygdala RVG expressing group showed higher speed
322 movement in OF compared the control (P < 0.001) and ΔRVG (P < 0.01) group (F (2,
323 16) = 17.99, P < 0.0001, Fig.7J). There was no significant difference in the velocity
324 between control and ΔRVG in the OF test.
325 Fig. 7K-N demonstrate EPM task of rats. One way ANOVA revealed a significant
326 difference in the time spent in the enclosed arms among groups (F (2, 16) = 6.248, P =
327 0.0099). RVG expression in amygdala enhanced the time elapsed in the enclosed arms
328 (P < 0.01 compared to the control group, Fig. 7K). However, no significant difference
329 was found between RVG and ΔRVG groups in the time spent in enclosed arms. RVG
330 group spent less time in the open arms (F (2, 16) = 5.163, P = 0.0186, Fig. 7K)
331 compared to the control and ΔRVG groups (P < 0.05). No significant difference was
332 found between control and ΔRVG groups. Intra-amygdala injection of RVG or ΔRVG did
333 not change percentage of enclosed and open arm entries (Fig. 7L). One way ANOVA
334 revealed significant difference in the total distance moved among groups (F (2, 16) =
335 24.28, P = 0.0186, Fig. 7M). Tukey post-test analysis indicated a significant difference in
336 the entire distance moved between RVG and control groups (P < 0.001, Fig. 7M). RVG-
337 expressing rats also travelled longer distance than ΔRVG group (P < 0.001) but no
338 difference was found between control and ΔRVG group. Intra-amygdala RVG
339 expressing rats also showed greater total number of arm entries (F (2, 15) = 9.991, P =

340 0.0017, Fig. 7N) compared to the control group ($P < 0.01$). No difference was found
341 between RVG and ΔRVG group.

342 **4. Discussion**

343 We found in this study that infecting hypothalamic, and amygdala neurons with RVG
344 induces anxiety-like behaviors in rats. PBM of RVG was involved in the observed
345 anxiety-like behaviors. Infection of hypothalamus and dorsal hippocampus was
346 accompanied by increase of serum corticosterone level indicating response of HPA axis
347 to RVG infection.

348 Animal and human findings indicate RABV markedly infects the brain regions involved
349 in anxiety, including hypothalamus (Preuss et al., 2009) hippocampus (Stein et al.,
350 2010; Song et al., 2013) and amygdala (Dolman and Charlton, 1987; Suja et al., 2011).
351 We found that infection of the PVN of hypothalamus by RVG increased OF parameters,
352 including the total distance moved and the velocity, and significantly decreased the time
353 spent in the open arms of EPM. Yet, the other index of anxiety in EPM, i.e., the number
354 of entries to the open arms was not changed. It is believed that the percentage of time
355 spent in the open arms is more indicative parameter compared to the number of entries,
356 and reflects increased aversion to the open arms due to increased fear or anxiety
357 (Pellow et al., 1985). Therefore, it seems that PVN infection with RVG induces both
358 anxiety-like behaviors and locomotor hyperactivity in rats. These behavioral changes
359 were not seen in the ΔRVG-infected rats, indicating involvement of PBM of RVG in the
360 both anxiety-like behaviors and locomotor hyperactivity. In addition, RVG but not ΔRVG
361 infection of the PVN was accompanied by HPA axis response. The corticotrophin-
362 releasing hormone (CRH) neurons are the main neural population in PVN. CRH

neurons have a major role in manifestation of anxiety-like behaviors. The selective deletion of CRH neurons in PVN markedly attenuates anxiety-like behaviors in mice in various models of anxiety including open field and EPM tests (Zhang et al., 2017). CRH fibers in PVN project widely to the brain regions with potential role in anxiety behaviors including cerebral cortex, amygdala, septum, bed nucleus of the stria terminalis, and accumbens nucleus (Zhang et al., 2017). Meanwhile, CRH neurons in PVN synchronize endocrine, autonomic, and behavioral responses to stress through direct control of HPA axis. CRH stimulates secretion of ACTH from anterior pituitary, which in turn promotes production and secretion of corticosteroids from the adrenal cortex into blood stream. Schutsky et al., (2014) reported a 12-fold increase in brain and serum corticosterone levels in RABV-infected mice. They concluded that activation of HPA axis contributes to pathogenesis of RABV (Schutsky et al., 2014). Intriguingly, in our study infecting PVN with ΔRVG did not increase serum corticosterone level. Therefore, the PBM of RVG might be responsible for the HPA axis activation observed in our study.

We have previously observed that infection of the dorsal hippocampus by RVG, increased fear-related memory in rats (Ghassemi et al., 2021b). Meanwhile, there are evidence indicating that regardless of the key role of the ventral hippocampus in the anxiety-like behaviors (Kjelstrup et al., 2002; Bannerman et al., 2004; McHugh et al., 2004) dorsal hippocampus also modifies emotional processes such as fear and anxiety behaviors (File et al., 2000; Solati et al., 2010). Therefore, it was interesting to witness anxiety-like behaviors of rats with dorsal hippocampus RVG infection. RVG infection of dorsal hippocampus did not alter the OF parameters of the locomotor activity. Yet, duration in the center zone and center to corners entrance ratio were significantly

386 reduced in the infected rats. It is shown in rodents that the time spent in the OF central
387 zone often positively correlates with the time spent in EPM open arms (Walf et al.,
388 2007). In our study, no significant difference in % time spent in and % entries to open
389 arms was observed between rats with dorsal hippocampus infection and the uninfected
390 control rats. Therefore, RVG did not induce anxiety-like behaviors in rats with dorsal
391 hippocampus infection. This finding might be due to the weak role of dorsal region of the
392 hippocampus in anxiety-related behaviors, and that the ventral hippocampus specifically
393 controls the fear and anxiety-like behaviors (Kjelstrup et al., 2002; Bannerman et al.,
394 2004; McHugh et al., 2004). In our study Both RVG and ΔRVG expression in dorsal
395 hippocampus was accompanied by significant increase in serum corticosterone level.
396 Therefore, it seems PBM of RVG is not involved in HPA axis response. Anatomical
397 (hippocampal projections to hypothalamus) and pharmacological (expression of
398 glucocorticoid receptors in the hippocampus) evidence (Jacobson and Sapolsky, 1991),
399 point out a dual (both negative and positive) role of hippocampus, as a regulator of HPA
400 axis response, depending on the ventral or dorsal hippocampus involvement. Ventral
401 hippocampus exerts an inhibitory influence on PVN and blunts HPA axis response to
402 the basal and stress-induced glucocorticoid levels (Jankord and Herman, 2008).
403 Whereas, electrical stimulation of dorsal CA1 hippocampal neurons increases plasma
404 corticosterone level in anesthetized (Dunn and Orr, 1984), as well as conscious non-
405 stressed (Casady and Taylor, 1976) rats. The different response of HPA to the dorsal
406 and ventral hippocampal stimulation is attributed to different efferent projections of
407 ventral and dorsal CA1 to the other brain regions (Casady and Taylor, 1976). Given the
408 crucial role of the ventral hippocampus in anxiety, measuring the anxiety-like behaviors

409 and HPA response after infection of ventral hippocampus with RVG is needed to further
410 elucidate how different parts of hippocampus interact with RVG.

411 In our study infection of amygdala by RVG increased the indicators of locomotor and
412 exploratory activities in both OF and EPM tests. These parameters were not changed in
413 rats with amygdala ΔRVG infection. Thus, it seems that similar to PVN, the positive
414 effect RVG on locomotor and exploratory activities of rats with amygdala infection is
415 also mediated via the PBM of RVG. Meanwhile, rats with amygdala RVG infection
416 stayed less time in the open arms of EPM compared to control and ΔRVG–infected rats.
417 On the other hand, no change in the number of entries to the open arms was observed.
418 Consistent with this finding, rats with RVG, but not ΔRVG, infection in amygdala spent
419 less time in the center zone of the OF task. Hence, it is suggested that infection of
420 amygdala by RVG induces anxiety-like behaviors through the PBM of RVG. In line with
421 our results, pharmacological studies in experimental animals suggest that activation of
422 BLA is anxiogenic, whereas its inhibition is anxiolytic (Truitt et al., 2009; Felix-Ortiz et
423 al., 2013, Prager et al., 2016). We found that infecting BLA neurons by RVG did not
424 promote HPA response and alteration in corticosterone serum level. It is well known that
425 electrical stimulation of the amygdala is associated with an increase in corticosteroid
426 secretion in humans and experimental animals (Jankord and Herman, 2008). There are
427 marked subregional differences within the amygdala in activating HPA axis. It is
428 believed that the central and medial amygdaloid nuclei intensify HPA axis responses to
429 acute stress. However, the BLA is involved in chronic stress, which depending on the
430 case, can either facilitate or inhibit the HPA axis response (Jankord and Herman, 2008;
431 Myers et al., 2012). Our finding of no change in corticosterone level of rats with RVG-

infection in BLA might be the outcome of both facilitation and inhibition of HPA response processes within BLA.

It is well known that RABV retains viability of the infected neurons via selective association of PBM of RVG with the PDZ domain of neuronal microtubule associated serine/threonine kinase (MAST) 2 (Terrien et al., 2012). In fact, MAST2 and PTEN (phosphatase and tensin homolog deleted on chromosome 10) negatively regulate cell survival pathways via formation of PTEN-MAST2 complex. The surface structure of PBM-RVG is largely similar to the carboxy-terminal PDZ domain-binding site of PTEN, and they compete with each other for binding to MAST2-PDZ. Ultimately, formation of the PTEN-MAST2 complex is disturbed by RVG and leads to neuronal survival (Terrien et al., 2012). Interestingly, it is reported that deletion of PTEN in somatostatin-expressing-GABAergic neurons impairs learning, and increases anxiety-like behaviors in mice in EPM and open field tests (Shin et al., 2021). It is not unlikely that expression of PBM-RVG in the brain regions involved in anxiety including hypothalamus, and amygdala could in the same way disrupt PTEN signaling pathways and result in anxiety-like behaviors in rats with RVG infection. Exploring the PDZ protein targets of PBM of RVG needs to be elucidated in future studies.

One of the most curious aspects in Rabies pathology is alterations in the function of infected neurons without any remarkable neuroinflammation and cell death (Baloul and Lafon, 2003; Scott et al., 2008; Lafon, 2011; Fooks and Jackson, 2020). These functional changes are attributed to impairment in the neurotransmission of mainly acetylcholine, serotonin and gamma-aminobutyric acid (GABA), as well as overproduction of nitric oxide (Fu and Jackson, 2005). Among the neurotransmitter

455 receptors, nicotinic acetylcholine receptors (nAChR) were the first receptors recognized
456 in RABV pathogenicity (Lentz et al., 1982). It is shown that a short region in the
457 ectodomain of RVG is able to inhibit α4β2 nAChR, the predominant subtype of nAChR
458 in CNS, and thereby increase locomotor activity of mice (Hueffer et al., 2017). This
459 study supports our finding on the increase locomotor activity of rats with RVG infection
460 in hypothalamus and amygdala. Meanwhile, the pivotal role of nAChRs containing α4β2
461 subunits in anxiety is established by several studies. It is shown that pharmacologic
462 activation of α4β2 nAChRs elicits anxiolytic behavior (Brioni et al., 1994), decreases
463 anxiogenic-like effect of nicotine withdrawal (Decker et al., 1994) and blocks anxiolytic
464 effect of nicotine administration (Decker et al., 1995) in EPM test. Abundant expression
465 of nAChRs and their contribution to HPA axis activity, stress and anxiety behavior are
466 well described for PVN of hypothalamus (Balkan and Pogun, 2018), dorsal
467 hippocampus (File et al., 2000), and BLA (Mineur et al., 2016; Sharp, 2019). Therefore,
468 blocking nAChRs function by RVG via its PBM might also play a role in the anxious-like
469 behaviors as well as the elevated locomotion of the RVG-infected rats in our study.

470 Nitric oxide (NO) is a gaseous signaling molecule and the key messenger of innate
471 immune system contributing to variety of physiological and pathophysiological
472 processes. Expression of inducible nitric oxide synthase (iNOS) gene and synthesis of
473 NO are strongly upregulated in the brain during RABV infection and implicated in clinical
474 signs and histopathological lesions of the infected rodents (Fu and Jackson, 2005). In
475 accordance with these findings, treatment of RABV-infected mice with a selective
476 inhibitor of iNOS significantly reduced viral load and apoptotic cells and delayed
477 development of clinical signs and the death of the infected mice (Fu and Jackson,

2005). On the other hand, several clues indicate potential role of NO in anxiety and HPA axis hyperactivity. NOS is expressed in brain areas involved in anxiety including amygdala, hippocampus and hypothalamus; and NO generation in these areas are accompanied by HPA axis hyperactivity (Zhou et al., 2018). In addition, pharmacological evidence indicate that overproduction of NO exerts anxiogenic effect in rodents (Zhou et al., 2018; Zhu et al., 2018). We did not measure NO level and NOS expression in the brain of the RVG-infected rats. However, it is likely that similar to RABV, RVG would also stimulate overexpression of NOS, leading to NO increase and anxiety behavior. Meanwhile, NOS possesses a PDZ domain interacting with other proteins. One of these proteins is a scaffolding protein known as carboxy-terminal PDZ ligand of NOS (CAPON), whose overexpression induces anxiety behaviors in mice in EPM test (Zhu et al., 2018). It is possible that PBM-RVG might act similar to CAPON, and interacts with PDZ domain of NOS, promoting anxiety in the RVG-infected rats. In support of this suggestion and considering the structure similarity between PBM-RVG and CAPON, it is known that CAPON regulates dendritic spine development, outgrowth and branching (Richier et al., 2010). Intriguingly, RVG and some peptides derived from RVG are also able to promote neurite outgrowth via their C-terminal PBM (Khan et al., 2019). Furthermore, electrophysiological evidence indicate that CAPON enhances synaptic functions of rat cortical neurons via changing spine numbers, morphology and maturation (Hernandez et al., 2016). In line with this report, we have also reported recently that RVG expression in rat hippocampal neurons increases synaptic plasticity (Ghassemi et al., 2021a). Biophysical and spectrometric studies are needed to examine

500 the extent of affinity and surface interaction of RVG and CAPON with PDZ domain of
501 NOS.

502 In conclusion, the results of the present study further expand our understanding of
503 RABV's ability to alter the mental status of the infected host by its glycoprotein spikes.
504 Anxiety disorders might be developed or provoked in the infected patient without any
505 characteristic symptoms of rabies. It is reported that rabies can be contracted to
506 humans by inconspicuous routes via wild animals or even asymptomatic pets, such as
507 through saliva drops entering the eye or nose, or animal licks on even minor scratches
508 and wounds; For instance, a difficult-to-diagnose case of rabies is reported in a patient
509 with a state of anxiety and depression without an apparent animal bite (Prabhakar and
510 Monsy Abraham, 2006). These inconspicuous routes of transfer and possible delayed
511 onset of severe symptoms, might lead to undiagnosed rabies cases in humans. On the
512 other hand, in recent years, some research is being conducted on possible agents and
513 protocols to prevent the fatal outcome of the rabies disease even in clinical stages; i.e.
514 when the RABV has infiltrated the nervous system and brain (El-Sayed, 2018).
515 Therefore, even later diagnosis of the disease and administration of recommended
516 protocols might save the patients. In cases of idiopathic anxiety, RABV infection can be
517 considered as a possible culprit, and it must not be overlooked and rabies diagnostic
518 tests are recommended. On the other hand, the prevalence and burden of anxiety
519 disorders (and mental disorders overall) have even increased in recent years after
520 emergence of the COVID-19 pandemic (COVID-19 Mental Disorders Collaborators,
521 2021). This growing trend necessitates discovery and development of new anti-anxiety
522 drugs more than before. Further studies on anxious-like effect of RVG and its PBM,

might open a new avenue in discovery of novel targets for development of new anxiolytic drugs.

Limitations

Our study has some limitations. We did not test effect of the empty vector, which is just expressing GFP, on the anxiety-like behaviors and serum corticosterone level. Since the PDZ binding domain is deleted in ΔRVG, it can be therefore regarded as the appropriate matched reference for RVG. Therefore, we used ΔRVG as the reference for RVG. Expression of ΔRVG in PVN of hypothalamus and BLA was not associated with significant change in the anxiety-like behaviors compared to the control group. RVG and ΔRVG expression in the dorsal hippocampus also did not change anxiety-like behaviors but increased corticosterone level. Yet, including an empty vector in the experimental groups should be taken into account for future studies.

The other limitation of our study is that it does not provide any information regarding the role of RVG in the fear-related behaviors. Although EPM is a model of defensive fear responses during exposure to a potentially threatening environment, it does not cover all aspects of fear-related behaviors. Hydrophobia is the most prominent feature of rabies. Role of RVG and its PBM in the fear-related behaviors needs to be assessed in the more specific animal models of fear.

CRediT authorship contribution statement

Study concept and design: HGP, and MS. Acquisition of data: SGH. Analysis and interpretation of data: HGP, and MS. Drafting of the manuscript: HGP, CP, ML, and MS. Experimental design and statistical analysis: HGP, and MS. Obtained funding: MS.

Administrative, technical, and material support: MS. Study supervision: HGP, and MS. All authors had full access to all the data in the study and take responsibility for the integrity of the data and the accuracy of the data analysis.

Conflict of interest

The authors have no conflict of interest to declare.

Funding

This work is part of the PhD dissertation of Soheil Ghassemi and supported by Pasteur Institute of Iran.

References

Albertini, A.A., Ruigrok, R.W., Blondel, D., 2011. Rabies virus transcription and replication. Adv. Virus. Res. 79, 1-22. https://doi.org/10.1016/B978-0-12-387040-7.00001-9.

Balkan, B., Pogun, S., 2018. Nicotinic cholinergic system in the hypothalamus modulates the activity of the hypothalamic neuropeptides during the stress response. Curr. Neuropharmacol. 16, 371-387. https://doi.org/10.2174/1570159X15666170720092442.

Baloul, L., Lafon M., 2003. Apoptosis and rabies virus neuroinvasion. Biochimie. 85 (8), 777-788. https://doi.org/10.1016/s0300-9084(03)00137-8.

Bannerman, D.M., Rawlins, J.N., McHugh, S.B., Deacon, R.M., Yee, B.K., Bast, T., Zhang, W.N., Pothuizen, H.H., Feldon, J., 2008. Regional dissociations within the hippocampus-memory and anxiety. Neurosci. Biobehav. Rev. 28, 273-283. https://doi.org/10.1016/j.neubiorev.2004.03.004.

Brioni, J.D., O'Neill, A.B., Kim, D.J., Buckley, M.J., Decker, M.W., Arneric, S.P., 1994. Anxiolytic-like effects of the novel cholinergic channel activator ABT-418. J. Pharmacol. Exp. Ther. 271, 353-361.

Casady, R.L., Taylor, A.N., 1976. Effect of electrical stimulation of the hippocampus upon corticosteroid levels in the freely-behaving, non-stressed rat. Neuroendocrinology 20, 68-78. https://doi.org/10.1159/000122470.

Decker, M.W., Anderson, D.J., Brioni, J.D., Donnelly-Roberts, D.L., Kang, C.H., O'Neill, A.B., Piattoni-Kaplan, M., Swanson, S., Sullivan, J.P., 1995. Erysodine, a competitive antagonist at neuronal nicotinic acetylcholine receptors. Eur. J. Pharmacol. 280, 79-89. https://doi.org/10.1016/0014-2999(95)00191-m.

Decker, M.W., Brioni, J.D., Sullivan, J.P., Buckley, M.J., Radek, R.J., Raszkiewicz, J.L., Kang, C.H., Kim, D.J., Giardina, W.J., Wasicak, J.T., 1994. (S)-3-methyl-5-(1-methyl-2-pyrrolidinyl) isoxazole (ABT 418): a novel cholinergic ligand with cognition-enhancing and anxiolytic activities: II. In vivo characterization. J. Pharmacol. Exp. Ther. 270, 319-328.

Dolman, C.L., Charlton, K.M., 1987. Massive necrosis of the brain in rabies. Can. J. Neurol. Sci. 14, 162-165. https://doi.org/10.1017/s0317167100026329.

Dunn, J.D., Orr, S.E., 1984. Differential plasma corticosterone responses to hippocampal stimulation. Exp. Brain. Res. 54, 1-6. https://doi.org/10.1007/BF00235813.

El-Sayed, A., 2018. Advances in rabies prophylaxis and treatment with emphasis on immunoresponse mechanisms. Int J Vet Sci Med. 6, 8–15. https://doi.org/10.1016/j.ijvsm.2018.05.001.

Felix-Ortiz, A.C., Beyeler, A., Seo, C., Leppla, C.A., Wildes, C.P., Tye, K.M., 2013. BLA to vHPC inputs modulate anxiety-related behaviors. Neuron 79, 658-664. https://doi.org/10.1016/j.neuron.2013.06.016.

589 File, S.E., Kenny, P.J., Cheeta, S., 2000. The role of the dorsal hippocampal serotonergic and
590 cholinergic systems in the modulation of anxiety. Pharmacol. Biochem. Behav. 66, 65-72.
591 https://doi.org/10.1016/s0091-3057(00)00198-2.

592 Fu, Z.F., Jackson, A.C., 2005. Neuronal dysfunction and death in rabies virus infection. J.
593 Neurovirol. 11, 101-106. https://doi.org/10.1080/13550280590900445.

594 Ghassemi, S., Asgari, T., Mirzapour-Delavar, H., Aliakbari, S., Pourbadie, H.G., Prehaud, C.,
595 Lafon, M., Gholami, A., Azadmanesh, K., Naderi, N., Sayyah, M., 2021a. Lentiviral
596 Expression of Rabies Virus Glycoprotein in the Rat Hippocampus Strengthens Synaptic
597 Plasticity. Cell. Mol. Neurobiol. https://doi.org/10.1007/s10571-020-01032-9.

598 Ghassemi, S., Asgari, T., Pourbadie, H.G., Prehaud, C., Lafon, M., Naderi, N., Gholami, A.,
599 Azadmanesh, K., Sayyah, M., 2021. Rabies virus glycoprotein enhances spatial memory via
600 the PDZ binding motif. J. Neurovirol. 2021b. https://doi.org/10.1007/s13365-021-00972-2.

601 Hernandez, K., Swiatkowski, P., Patel, M.V., Liang, C., Dudzinski, N.R., Brzustowicz, L.M.,
602 Firestein, B.L., 2016. Overexpression of isoforms of nitric oxide synthase 1 adaptor protein,
603 encoded by a risk gene for schizophrenia, alters actin dynamics and synaptic function. Front.
604 Cell. Neurosci. 10, 6. https://doi.org/10.3389/fncel.2016.00006.

605 Hueffer, K., Khatri, S., Rideout, S., Harris, M.B., Papke, R.L., Stokes, C., Schulte, M.K., 2017.
606 Rabies virus modifies host behaviour through a snake-toxin like region of its glycoprotein that
607 inhibits neurotransmitter receptors in the CNS. Sci. Rep. 7, 12818.
608 https://doi.org/10.1038/s41598-017-12726-4.

609 Jacobson, L., Sapolsky, R., 1991. The role of the hippocampus in feedback regulation of the
610 hypothalamic-pituitary-adrenocortical axis. Endocr. Rev. 12, 118-134.
611 https://doi.org/10.1210/edrv-12-2-118.

612 Jankord, R., Herman, J.P., 2008. Limbic regulation of hypothalamo-pituitary-adrenocortical
613 function during acute and chronic stress. Ann. N. Y. Acad. Sci. 1148, 64-73.
614 https://doi.org/10.1196/annals.1410.012

615 Javier, R.T., Rice, A.P., 2011. Emerging theme: cellular PDZ proteins as common targets of
616 pathogenic viruses. J. Virol. 85, 11544-11556. https://doi.org/10.1128/JVI.05410-11.

617 Kennedy, M.B., 1995. Origin of PDZ (DHR, GLGF) domains. Trends Biochem. Sci. 20 (9), 350.
618 https://doi.org/10.1016/s0968-0004(00)89074-x.

619 Khan, Z., Terrien, E., Delhommel, F., Lefebvre-Omar, C., Bohl, D., Vitry, S., Bernard, C.,
620 Ramirez, J., Chaffotte, A., Ricquier, K., Vincentelli, R.., Buc, H., Prehaud, C., Wolff, N., Lafon,
621 M., 2019. Structure-based optimization of a PDZ-binding motif within a viral peptide
622 stimulates neurite outgrowth. J. Biol. Chem. 294, 13755-13768.
623 https://doi.org/10.1074/jbc.RA119.008238.

624 Kjelstrup, K.G., Tuvnes, F.A., Steffenach, H.A., Murison, R., Moser, E.I., Moser, M.B., 2002.
625 Reduced fear expression after lesions of the ventral hippocampus. Proc. Natl. Acad. Sci. 99
626 (16), 10825-10830. https://doi.org/10.1073/pnas.152112399.

627 Koury, R., Warrington, S.J., Rabies. 2020. In: StatPearls [Internet]. Treasure Island (FL):
628 StatPearls Publishing; 2021.

629 Lafon, M., 2011. Evasive strategies in rabies virus infection. Adv. Virus. Res. 79, 33-53.
630 https://doi.org/10.1016/B978-0-12-387040-7.00003-2.

631 Lentz, T.L., Burrage, T.G., Smith, A.L., Crick, J., Tignor, G.H., 1982. Is the acetylcholine
632 receptor a rabies virus receptor? Science 215, 182-184.
633 https://doi.org/10.1126/science.7053569.

634 Lindtjørn, B., 1982. Clinical features of rabies in man. Trop. Doct. 12 (1), 9-12.
635 https://doi.org/10.1177/004947558201200104.

636 Martin, E.I., Ressler, K.J., Binder, E., Nemeroff, C.B., 2009. The neurobiology of anxiety
637 disorders: brain imaging, genetics, and psychoneuroendocrinology. Psychiatr. Clin. North.
638 Am. 32, 549-575. https://doi.org/10.1016/j.psc.2009.05.004.

639 McHugh, S.B., Deacon, R.M., Rawlins, J.N., Bannerman, D.M., 2004. Amygdala and ventral
640 hippocampus contribute differentially to mechanisms of fear and anxiety. Behav. Neurosci.
641 118 (1), 63-78. https://doi.org/10.1037/0735-7044.118.1.63.

642 Mental Disorders Collaborators, 2021. Global prevalence and burden of depressive and anxiety
643 disorders in 204 countries and territories in 2020 due to the COVID-19 pandemic. Lancet 98,
644 1700–1712. https://doi.org/10.1016/S0140-6736 (21)02143-7.

645 Mineur, Y.S., Fote, G.M., Blakeman, S., Cahuzac, E.L., Newbold, S.A., Picciotto, M.R., 2015.
646 Multiple nicotinic acetylcholine receptor subtypes in the mouse amygdala regulate affective
647 behaviors and response to social stress. Neuropsychopharmacology 41, 1579-1587.
648 https://doi.org/10.1038/npp.2015.316.

649 Mitrabhakdi, E., Shuangshoti, S., Wannakrairot, P., Lewis, R. A., Susuki, K., Laothamatas, J.,
650 Hemachudha, T., 2005. Difference in neuropathogenetic mechanisms in human furious and
651 paralytic rabies. J. Neurol. Sci. 238 (1-2), 3–10. https://doi.org/10.1016/j.jns.2005.05.004

652 Myers, B., McKlveen, J.M., Herman, J.P., 2012. Neural regulation of the stress Response: The
653 many faces of feedback. Cell. Mol. Neurobiol. https://doi.org/10.1007/s10571-012-9801-y.

654 Paxinos, G., Watson, C., 2006. The rat brain in stereotaxic coordinates. Hard cover edition.
655 Academic Press.

656 Pellow, S., Chopin, P., File, S.E., Briley, M., 1985. Validation of open:closed arm entries in an
657 elevated plus-maze as a measure of anxiety in the rat. J. Neurosci. Methods. 14 (3),149-167.
658 https://doi.org/10.1016/0165-0270(85)90031-7.

659 Prager, E.M., Bergstrom, H.C., Wynn, G.H., Braga, M.F., 2016. The basolateral amygdala γ-
660 aminobutyric acidergic system in health and disease. J. Neurosci. Res. 94, 548-567.
661 https://doi.org/10.1002/jnr.23690.

662 Prabhakar, V.R., Monsy Abraham, R.N., 2006. A case of difficult diagnosis of rabies in the
663 absence of a dog bite in a patient with depression. J. Neuropsychiatry. Clin. Neurosci. 18,
664 425–426. https://doi.org/10.1176/jnp.2006.18.3.425

665 Preuss, M.A.R., Faber, M.L., Tan, G.S., Bette, M., Dietzschold, B., Weihe, E., Schnell. M.J.,
666 2009. Intravenous inoculation of a Bat-associated Rabies virus causes lethal encephalopathy
667 in mice through invasion of the brain via neurosecretory hypothalamic fibers. PLoS Pathog. 5,
668 e1000485. https://doi.org/10.1371/journal.ppat.1000485.

669 Richier, L., Williton, K., Clattenburg, L., Colwill, K., O'Brien, M., Tsang, C., Kolar, A., Zinck, N.,
670 Metalnikov, P., Trimble, W.S., Krueger, S.R., Pawson, T., Fawcett, J.P., 2010. NOS1AP
671 associates with Scribble and regulates dendritic spine development. J. Neurosci. 30, 4796-
672 4805. https://doi.org/10.1523/JNEUROSCI.3726-09.2010.

673 Rossiter, J.P., Jackson, A.C. (2020). Pathology. In Rabies: Basis of the Disease and Its
674 Management, A.R. Fooks, A.C. Jackson, eds. (Academic Press, Elsevier), pp. 347-387.

675 Rupprecht, C.E., 1996. Rhabdoviruses: Rabies Virus. In: Baron S, Medical Microbiology.
676 Galveston (TX): University of Texas Medical Branch at Galveston.

677 Saras, J., Heldin, C.H., 1996. PDZ domains bind carboxy-terminal sequences of target proteins.
678 Trends Biochem. Sci. 21, 455-458. https://doi.org/10.1016/s0968-0004(96)30044-3.

679 Schutsky, K., Portocarrero, C., Hooper, D.C., Dietzschold, B., Faber, M., 2014. Limited brain
680 metabolism changes differentiate between the progression and clearance of rabies
681 virus. PLoS One. 9, e87180. https://doi.org/10.1371/journal.pone.0087180.

682 Scott, C.A., Rossiter, J.P., Andrew, R.D., Jackson, A.C., 2008. Structural abnormalities in
683 neurons are sufficient to explain the clinical disease and fatal outcome of experimental rabies
684 in yellow fluorescent protein-expressing transgenic mice. J. Virol. 82 (1), 513-521.
685 https://doi.org/10.1128/JVI.01677-07.

686 Shin, S., Santi, A., Huang, S., 2021. Conditional Pten knockout in parvalbumin- or somatostatin-
687 positive neurons sufficiently leads to autism-related behavioral phenotypes. Mol. Brain. 14,
688 24. https://doi.org/10.1186/s13041-021-00731-8.

689 Solati, J., Zarrindast, M.R., Salari, A.A., 2010. Dorsal hippocampal opioidergic system
690 modulates anxiety-like behaviors in adult male Wistar rats. Psychiatry Clin. Neurosci. 64,
691 634-641. https://doi.org/10.1111/j.1440-1819.2010.02143.x.

692 Song, Y., Hou, J., Qiao, B., Li, Y., Xu, Y., Duan, M., Guan, Z., Zhang, M., Sun, L., 2013. Street
693 rabies virus causes dendritic injury and F-actin depolymerization in the hippocampus. J. Gen.
694 Virol. 94, 276-283. https://doi.org/10.1099/vir.0.047480-0.

695 Steimer, T., 2002. The biology of fear- and anxiety-related behaviors. Dialogues Clin. Neurosci.
696 4, 231-249. https://doi.org/10.31887/DCNS.2002.4.3/tsteimer.

Stein, L.T., Rech, R.R., Harrison, L., Brown, C.C., 2010. Immunohistochemical study of rabies virus within the central nervous system of domestic and wildlife species. Vet. Pathol. 47, 630-633. https://doi.org/10.1177/0300985810370013.

Suja, M.S., Mahadevan, A., Madhusudana, S.N., Shankar, S.K., 2011. Role of apoptosis in rabies viral encephalitis: a comparative study in mice, canine, and human brain with a review of literature. Patholog. Res. Int. 374286. https://doi.org/10.4061/2011/374286.

Terrien, E., Chaffotte, A., Lafage, M., Khan, Z., Préhaud, C., Cordier, F., Simenel, C., Delepierre, M., Buc, H., Lafon, M., Wolff, N., 2012. Interference with the PTEN-MAST2 interaction by a viral protein leads to cellular relocalization of PTEN. Sci. Signal. 5, ra58. https://doi.org/10.1126/scisignal.2002941.

Tordo, N., Kouknetzoff, A., 1993. The rabies virus genome: an overview. Onderstepoort. J. Vet. Res. 60 (4), 263-269.

Truitt, W.A., Johnson, P.L., Dietrich, A.D., Fitz, S.D., Shekhar, A., 2009. Anxiety-like behavior is modulated by a discrete subpopulation of interneurons in the basolateral amygdala. Neuroscience 160, 284-294. https://doi.org/10.1016/j.neuroscience.2009.01.083.

Walf, A.A., Frye, C.A., 2007. The use of the elevated plus maze as an assay of anxiety-related behavior in rodents. Nat. Protoc. 2 (2), 322-328. https://doi.org/10.1038/nprot.2007.44.

Zhang, R., Asai, M., Mahoney, C.E., Joachim, M., Shen, Y., Gunner, G., Majzoub, J.A., 2017. Loss of hypothalamic corticotropin-releasing hormone markedly reduces anxiety behaviors in mice. Mol. Psychiatry. 22, 733-744. https://doi.org/10.1038/mp.2016.136.

Zhou, Q.G., Zhu, X.H., Nemes, A.D., Zhu, D.Y., 2018. Neuronal nitric oxide synthase and affective disorders. IBRO Rep. 5, 116-132. https://doi.org/10.1016/j.ibror.2018.11.004.

Zhu, L.J., Ni, H.Y., Chen, R., Chang, L., Shi, H.J., Qiu, D., Zhang, Z., Wu, D.L., Jiang, Z.C., Xin, H.L., Zhou, Q.G., Zhu, D.Y., 2018. Hippocampal nuclear factor kappa B accounts for stress-induced anxiety behaviors via enhancing neuronal nitric oxide synthase (nNOS)-carboxy-terminal PDZ ligand of nNOS-Dexras1 coupling. J. Neurochem. 146, 598-612. https://doi.org/10.1111/jnc.14478.

Figures caption

Fig. 1. Structures of RVG and ΔRVG peptides.

The full-length RABV G-protein (RVG) is a 524-aa type I glycoprotein. RVG is attached to the endoplasmic reticulum (ER) and plasma membranes via its unique transmembrane domain (TM) and signal peptide (SP). The ectodomain (EC) of the G-protein is located within the luminal compartment of the ER initially, and then at the cell surface after fusion to the plasma membrane. During G-protein trafficking from the ER to the plasma membrane, the cytoplasmic

732 domain (Cyto) containing the C-terminal PBM is always exposed to the cytoplasm of the
733 somato-dendritic neuronal area, where it can interact with cellular partners. ΔRVG is generated
734 by deleting four amino acids of the C-terminal PBM-RVG (Khan et al., 2019). The image is from
735 Ghassemi et al., 2021b.

736 **Fig. 2.** Schematic representation of experimental timeline of the behavioral, histological and
737 biochemical assays. EPM: Elevated Plus Maze, OF: Open-Field, HPA: Hypothalamus-Pituitary-
738 Adrenal axis.

739 **Fig. 3.** Impact of caffeine on indices of the elevated plus maze and response of hypothalamus-
740 pituitary-adrenal axis in rats. Data are expressed as Mean ± SEM, and analyzed by the Un-
741 paired student's t-test. The data of corticosterone level were analyzed by the nonparametric
742 Kruskal-Wallis test. *P < 0.05, **P < 0.01, and ***P < 0.001 compared to corresponding control
743 group.

744 **Fig. 4.** Effect of RVG or ΔRVG expression in the hypothalamic paraventricular nucleus of rats
745 on the open field and elevated plus maze tasks, as well as serum corticosterone level one week
746 after microinjection of the lentiviral vectors containing RVG or ΔRVG. A: Schematic loci of
747 hypothalamic paraventricular nucleus is shown in the red box. B-C and D-E show representative
748 fluorescent green cells indicate RVG/GFP and ΔRVG/GFP expression, respectively, in neurons
749 of hypothalamic paraventricular nucleus one week after microinjection of the lentiviral vectors
750 containing RVG or ΔRVG. Magnification: 10x (B) and 20x (C), scale bar: 50 µm. F: The serum
751 level of corticosterone one week after injection of the lentivectors. G-J: The open field data one
752 week after injection of the lentivectors. K-N: The elevated plus maze data one week after
753 injection of the lentivectors. Data are expressed as Mean ± SEM and analyzed by one-way
754 ANOVA and Tukey post-hoc test. The data of corticosterone level were analyzed by the
755 nonparametric Kruskal-Wallis test. *P < 0.05, **P < 0.01, and ***P < 0.001 compared to
756 corresponding control group. ^^P < 0.01 and ^^^P < 0.001 compared to the RVG group.

Fig. 5. Effect of RVG or ΔRVG expression in the hypothalamic paraventricular nucleus of rats on the open field and elevated plus maze tasks, as well as serum corticosterone level two weeks after microinjection of the lentiviral vectors containing RVG or ΔRVG. A-B and C-D show representative fluorescent green cells indicate RVG/GFP and ΔRVG/GFP expression, respectively, in neurons of hypothalamic paraventricular nucleus two weeks after microinjection of the lentiviral vectors containing RVG or ΔRVG. Magnification: 10x (B) and 20x (C), scale bar: 50 µm. E-H: the open field data, and I-L: the elevated plus maze indices two weeks after injection of the lentivectors. Data are expressed as Mean ± SEM and analyzed by one-way ANOVA and Tukey post-hoc test. *P < 0.05, **P < 0.01, and ***P < 0.001 compared to corresponding control group. ^^^P < 0.001 compared to the RVG group.

Fig. 6. Effect of RVG or ΔRVG expression in the dorsal hippocampus of rats on the open field and elevated plus maze tasks, as well as serum corticosterone level. A: Schematic loci of dorsal hippocampus is shown in the red box. B-C and D-E show representative fluorescent green cells indicate RVG/GFP and ΔRVG/GFP expression, respectively, in neurons of dorsal hippocampus one week after microinjection of the lentiviral vectors containing RVG or ΔRVG. Magnification: 10x (B) and 20x (C), scale bar: 50 µm. F: The serum level of corticosterone one week after injection of the lentivectors. G-J: The open field data one week after injection of the lentivectors. K-N: The elevated plus maze data one week after injection of the lentivectors. Data are expressed as Mean ± SEM and analyzed by one-way ANOVA and Tukey post-hoc test. *P < 0.05, **P < 0.01, and ***P < 0.001 compared to corresponding control group. ^^^P < 0.001 compared to the RVG group.

Fig. 7. Effect of RVG or ΔRVG expression in the basolateral amygdala of rats on the open field and elevated plus maze tasks, as well as serum corticosterone level. A: Schematic loci of basolateral amygdala is shown in the red box. B-C and D-E show representative fluorescent green cells indicate RVG/GFP and ΔRVG/GFP expression, respectively, in neurons of basolateral amygdala one week after microinjection of the lentiviral vectors containing RVG or

ΔRVG. Magnification: 10x (B) and 20x (C), scale bar: 50 µm. F: The serum level of corticosterone one week after injection of the lentivectors. G-J: The open field data one week after injection of the lentivectors. K-N: The elevated plus maze data one week after injection of the lentivectors. Data are expressed as Mean ± SEM and analyzed by one-way ANOVA and Tukey post-hoc test. The data of corticosterone level were analyzed by the nonparametric Kruskal-Wallis test. *P < 0.05, **P < 0.01, and ***P < 0.001 compared to corresponding control group. ^P < 0.05, ^^P < 0.01 and ^^^P < 0.001 compared to the RVG group.

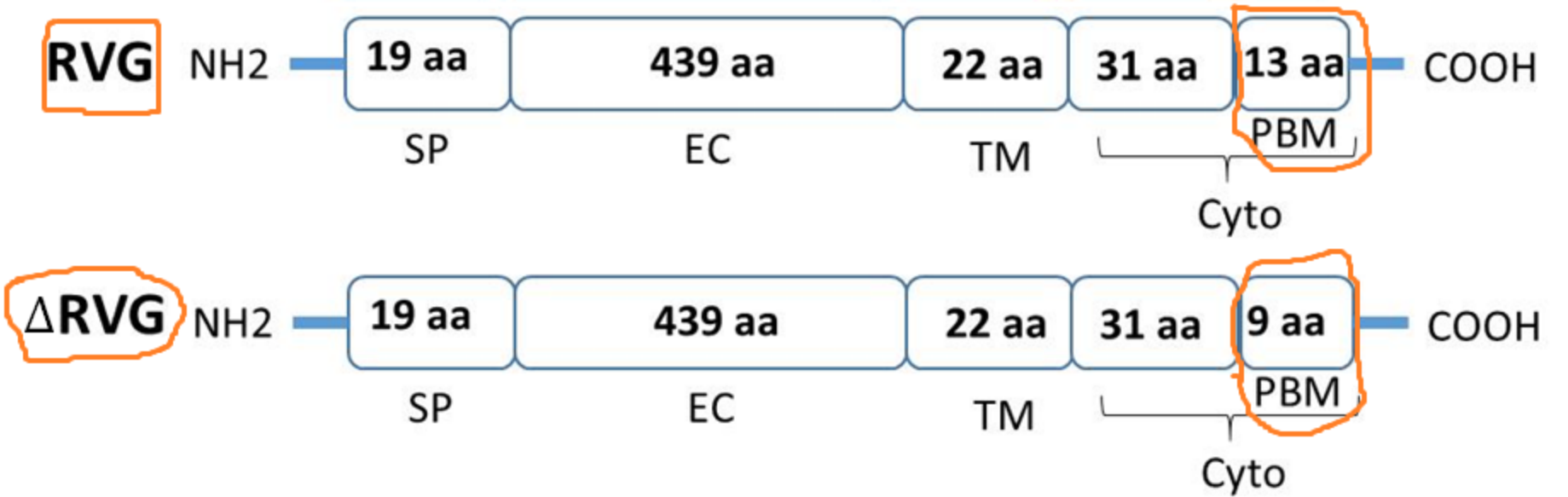
RVG
NH2
19 aa
439 aa
22 aa
31 aa
13 aa
COOH
SP
EC
TM
PBM
Cyto
ΔRVG
NH2
19 aa
439 aa
22 aa
31 aa
9 aa
COOH
SP
EC
TM
PBM
Cyto

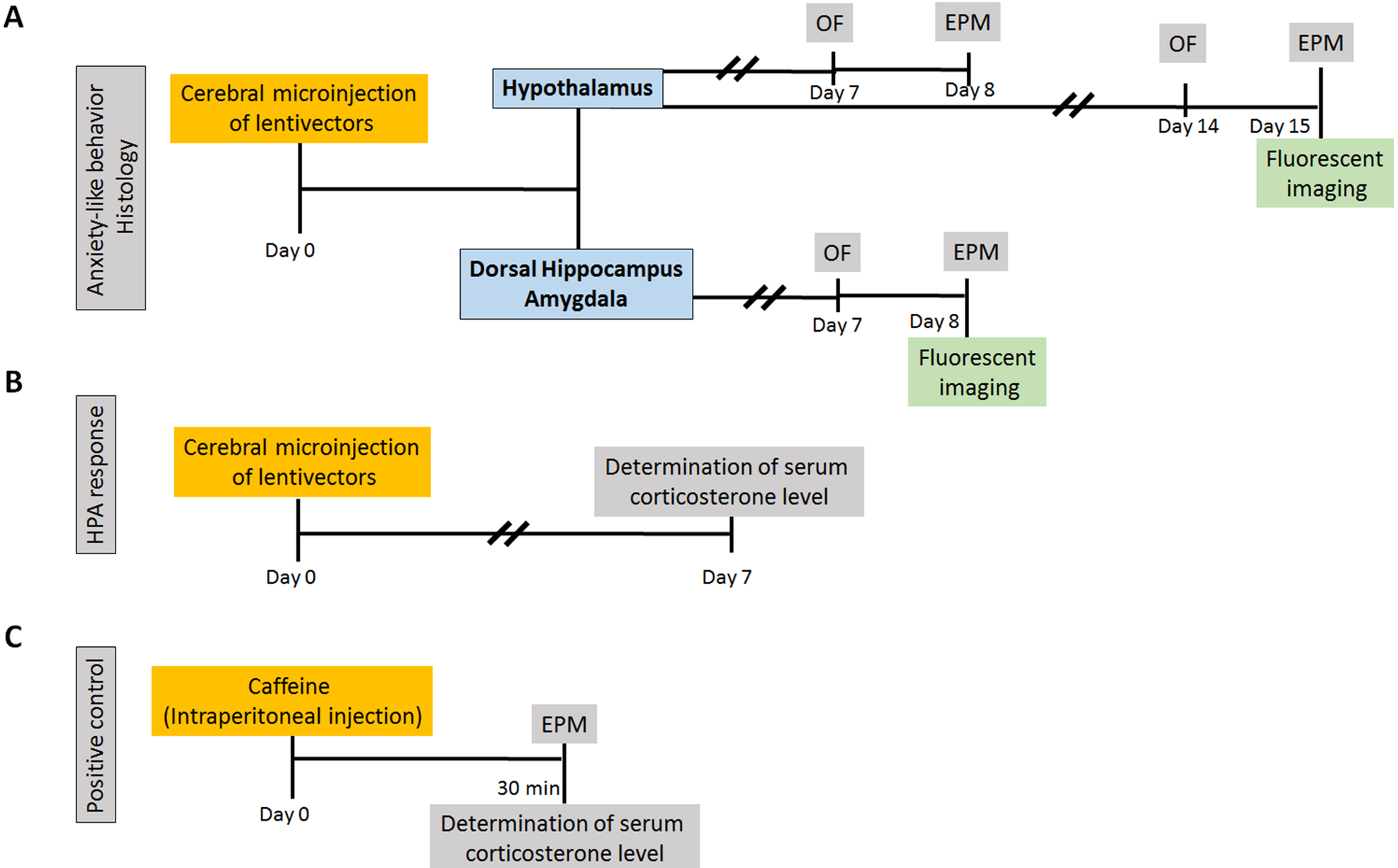
A
Anxiety-like behavior
Histology
Cerebral microinjection
of lentivectors
Day 0
Hypothalamus
OF
EPM
Day 7
Day 8
OF
EPM
Day 14
Day 15
Fluorescent
imaging
Dorsal Hippocampus
Amygdala
OF
EPM
Day 7
Day 8
Fluorescent
imaging
B
HPA response
Cerebral microinjection
of lentivectors
Day 0
Determination of serum
corticosterone level
Day 7
C
Positive control
Caffeine
(Intraperitoneal injection)
Day 0
EPM
30 min
Determination of serum
corticosterone level

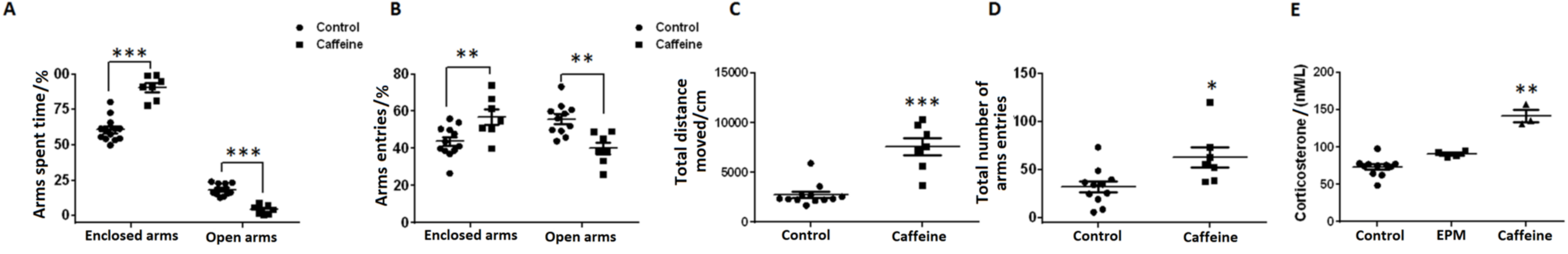
A
Control
Caffeine
Arms spent time/%
00
75
50
25
0
***
***
Enclosed arms
Open arms
B
Control
Caffeine
Arms entries/%
80
60
40
20
0
**
**
Enclosed arms
Open arms
C
Total distance moved/cm
15000
10000
5000
0
***
Control
Caffeine
D
Total number of arms entries
150
100
50
0
*
Control
Caffeine
E
Corticosterone/(nM/L)
200
150
100
50
0
**
Control
EPM
Caffeine

A

AP= −1.7, ML= ± 0.4, DV= −7.8

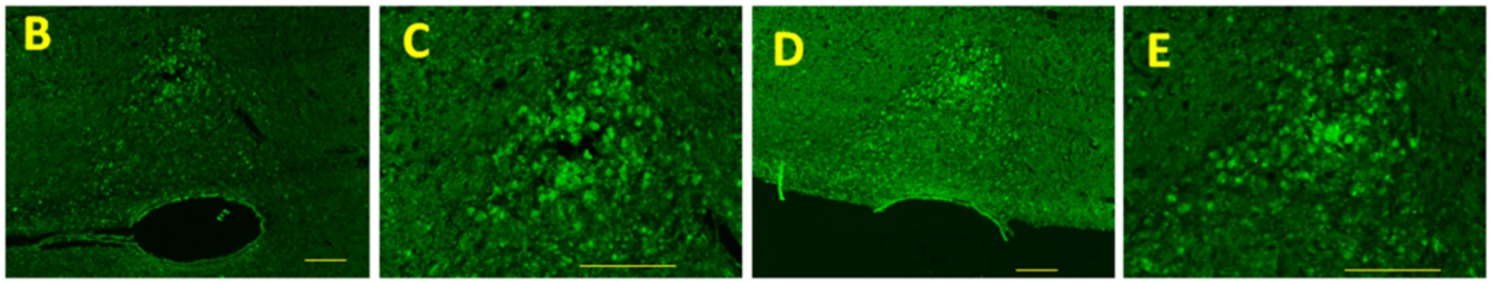

F

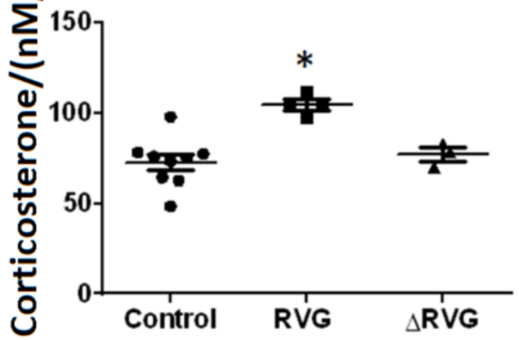

Day 7 post-infection

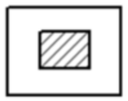

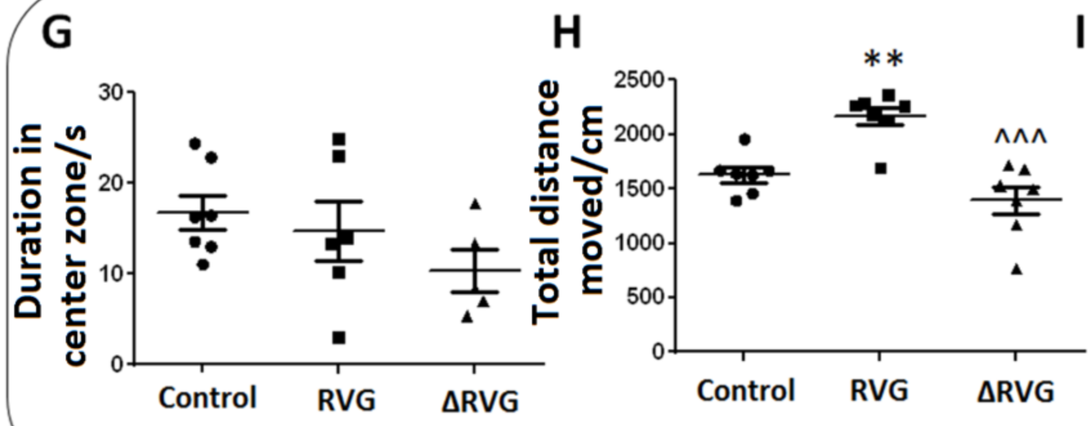

Day 7 post-infection

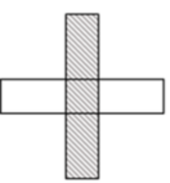

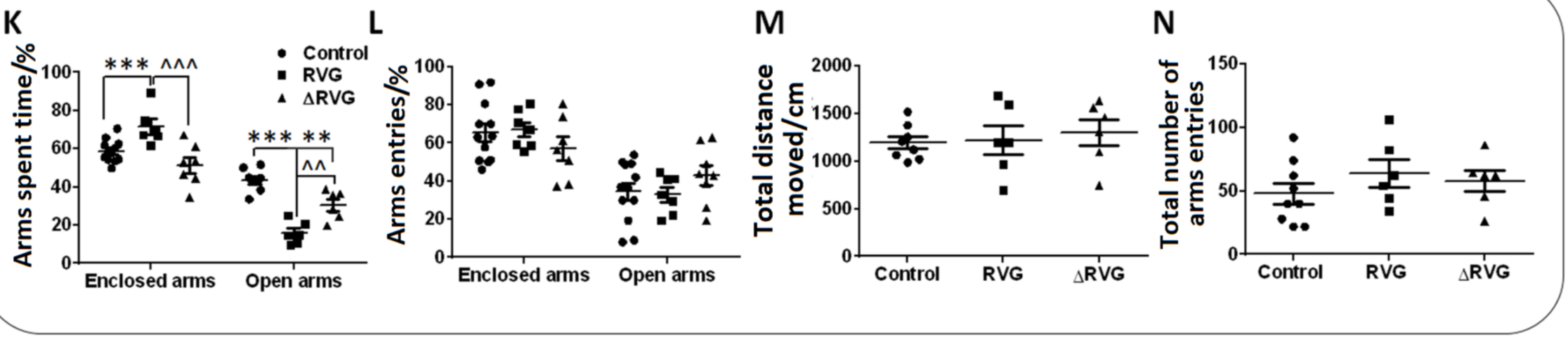

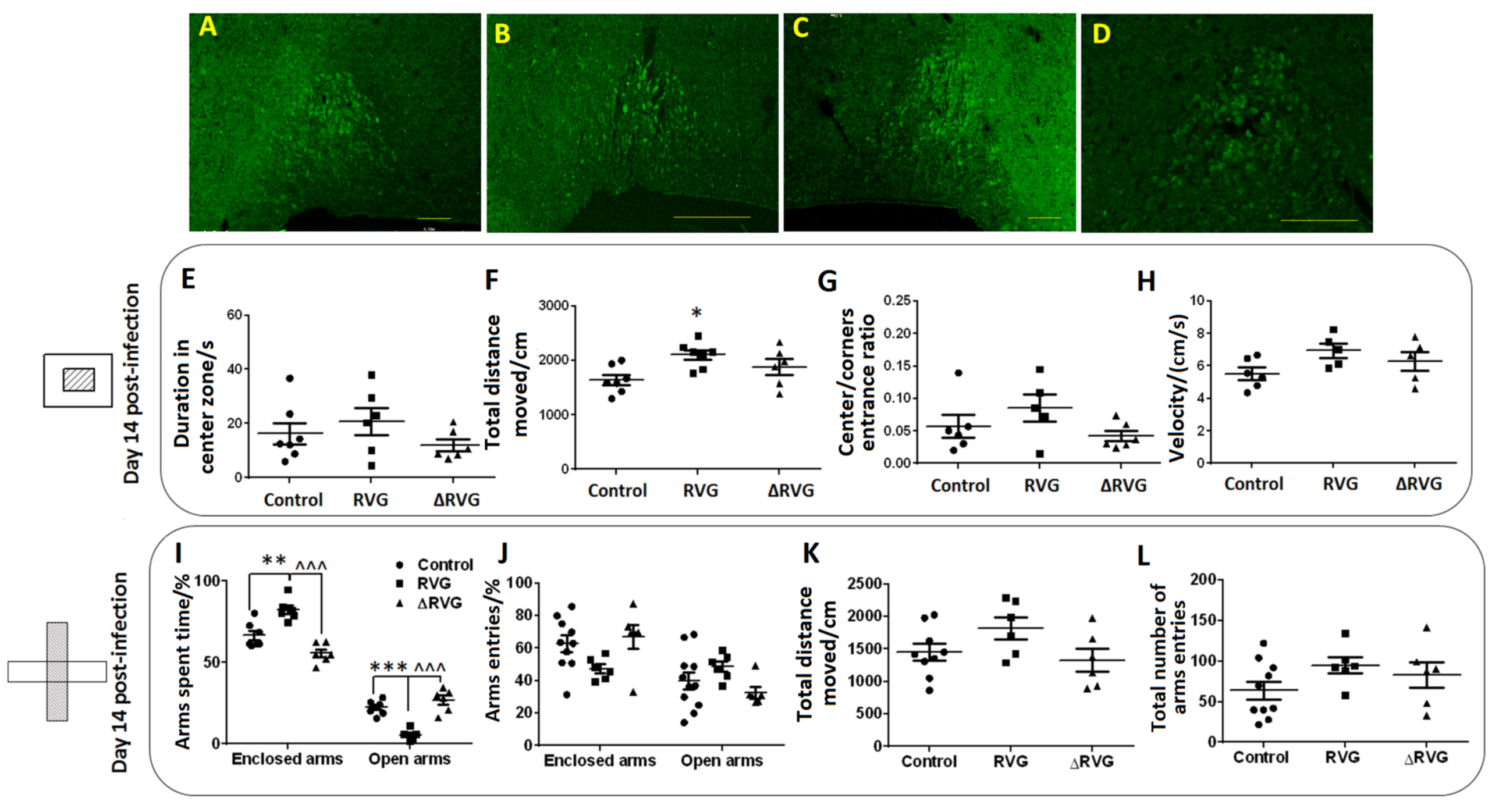
A
B
C
D
Day 14 post-infection
E
Duration in center zone/s
60
40
20
0
Control
RVG
ΔRVG
F
Total distance moved/cm
3000
2000
1000
0
*
Control
RVG
ΔRVG
G
Center/corners entrance ratio
0.25
0.20
0.15
0.10
0.05
0.00
Control
RVG
ΔRVG
H
Velocity/(cm/s)
10
8
6
4
2
0
Control
RVG
ΔRVG
Day 14 post-infection
I
Arms spent time/%
100
50
0
** ^^^
*** ^^^
Control
RVG
ΔRVG
Enclosed arms
Open arms
J
Arms entries/%
100
80
60
40
20
0
Enclosed arms
Open arms
K
Total distance moved/cm
2500
2000
1500
1000
500
0
Control
RVG
ΔRVG
L
Total number of arms entries
200
150
100
50
0
Control
RVG
ΔRVG

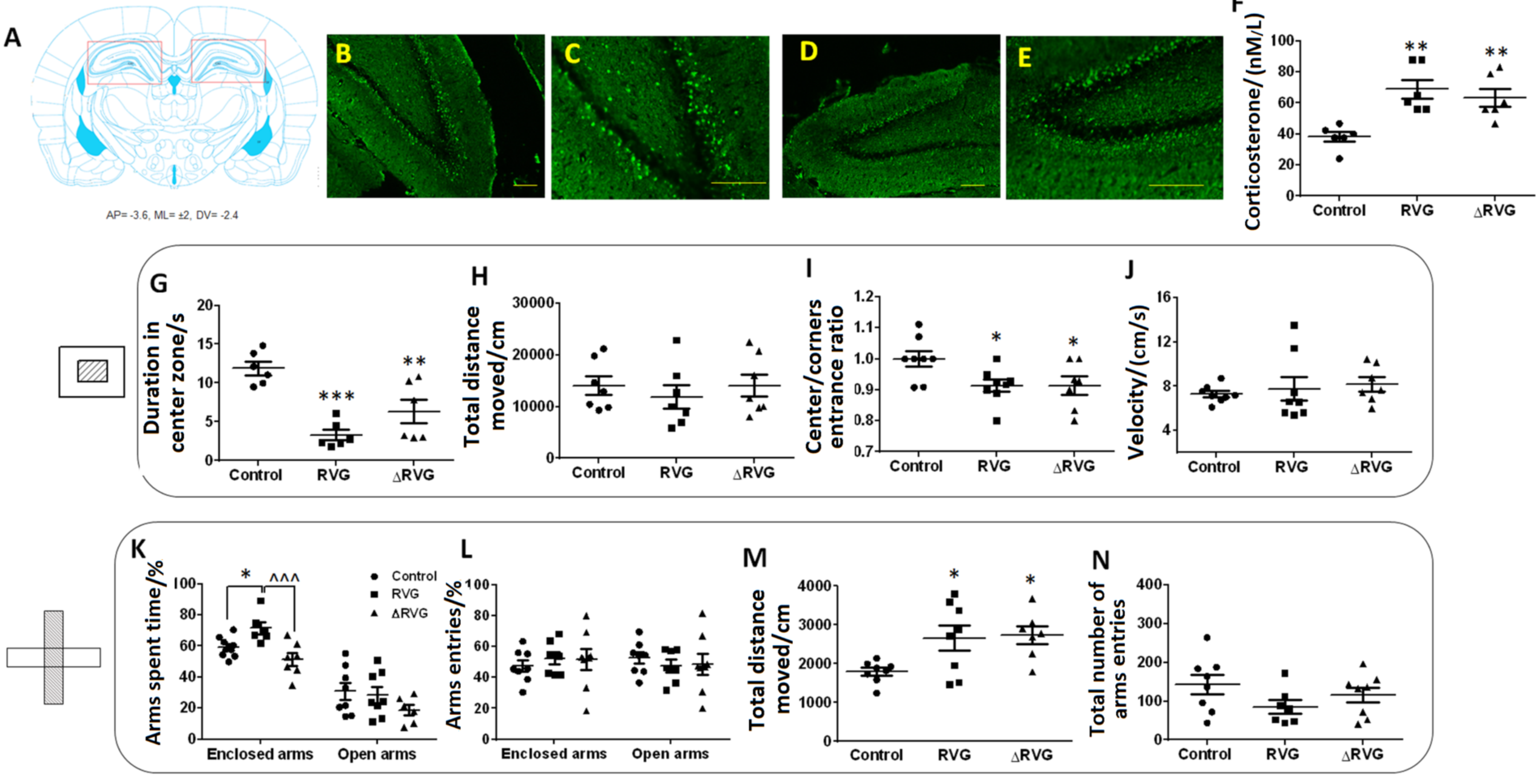
A
AP= -3.6, ML= ±2, DV= -2.4
B
C
D
E
F
Corticosterone/(nM/L)
100
80
60
40
20
0
**
**
Control
RVG
ΔRVG
G
Duration in center zone/s
20
15
10
5
0
***
**
Control
RVG
ΔRVG
H
Total distance moved/cm
30000
20000
10000
0
Control
RVG
ΔRVG
I
Center/corners entrance ratio
1.2
1.1
1.0
0.9
0.8
0.7
*
*
Control
RVG
ΔRVG
J
Velocity/(cm/s)
16
12
8
4
Control
RVG
ΔRVG
K
Arms spent time/%
100
80
60
40
20
0
*
^^^
Control
RVG
ΔRVG
Enclosed arms
Open arms
L
Arms entries/%
100
80
60
40
20
0
Enclosed arms
Open arms
M
Total distance moved/cm
4000
3000
2000
1000
0
*
*
Control
RVG
ΔRVG
N
Total number of arms entries
400
300
200
100
0
Control
RVG
ΔRVG

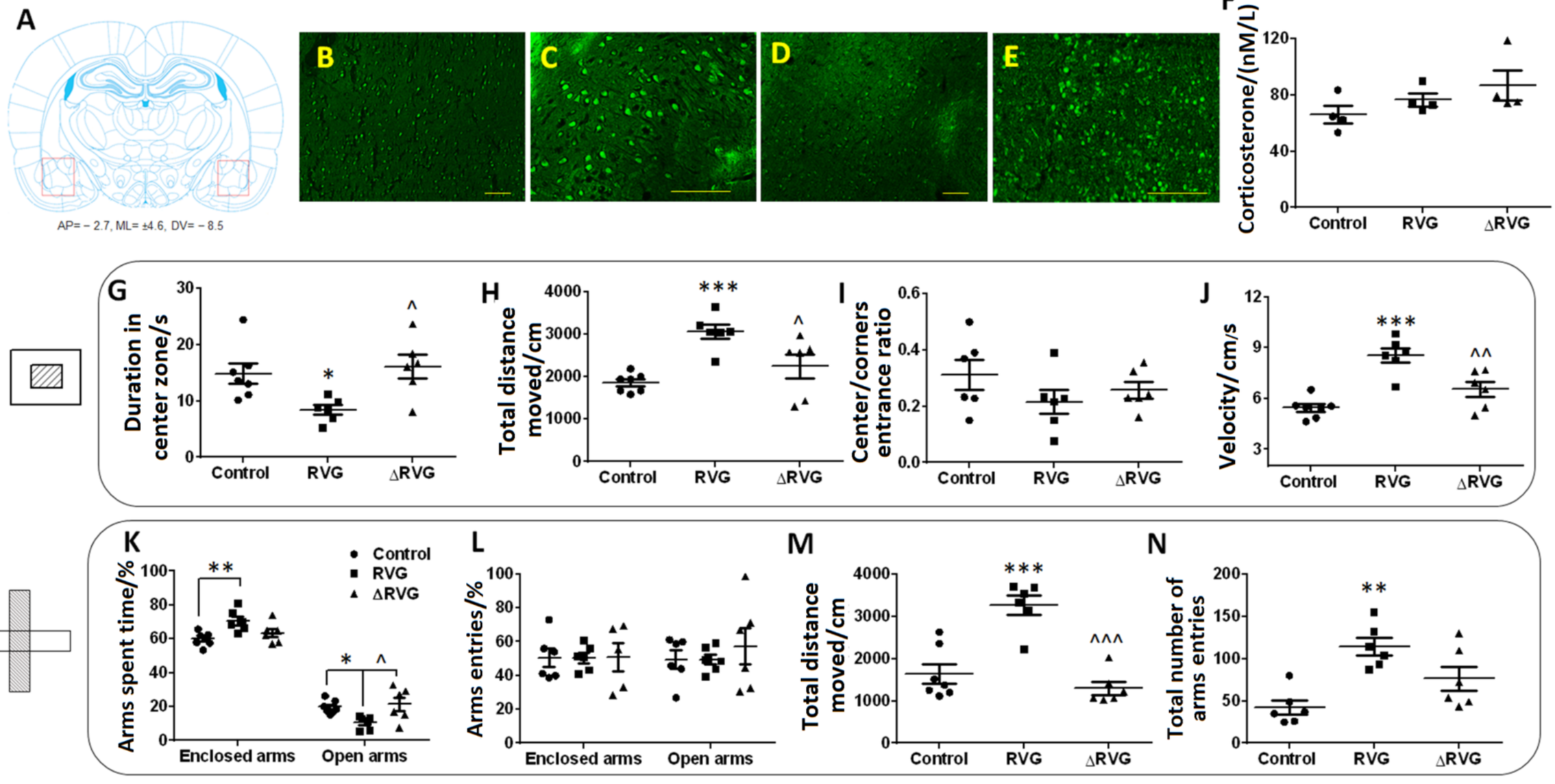
A
AP= – 2.7, ML= ±4.6, DV= – 8.5
B
C
D
E
F
Corticosterone/(nM/L)
120
80
40
0
Control
RVG
ΔRVG
G
Duration in center zone/s
30
20
10
0
*
^
H
Total distance moved/cm
4000
3000
2000
1000
0
***
^
I
Center/corners entrance ratio
0.6
0.4
0.2
0.0
J
Velocity/cm/s
12
9
6
3
***
^^
K
Arms spent time/%
100
80
60
40
20
0
**
*
^
Control
RVG
ΔRVG
Enclosed arms
Open arms
L
Arms entries/%
M
Total distance moved/cm
***
^^^
N
Total number of arms entries
200
150
100
50
**